Inner-shell electron-impact ionization of neutral atoms

J. Colgan,[1] C. J. Fontes,[2] and H. L. Zhang[2]
[1]*Theoretical Division, Los Alamos National Laboratory, Los Alamos, New Mexico 87545, USA*
[2]*Applied Physics Division, Los Alamos National Laboratory, Los Alamos, New Mexico 87545, USA*
(Received 17 April 2006; published 14 June 2006)

A study of inner-shell electron-impact ionization of heavy neutral atoms is presented. A relativistic distorted-wave method is used to calculate *K*-shell ionization of neutral Mn, Fe, Ni, and Cu, and also the *L*-shell ionization of neutral W. These calculations are compared with measurements made by electron-impact ionization from a thin target of the atomic species in question. Good agreement is found between the calculations and measurements.

DOI: 10.1103/PhysRevA.73.062711 PACS number(s): 34.80.Dp

I. INTRODUCTION

There has recently been considerable effort in measuring inner-shell ionization cross sections for heavy neutral targets. Such cross sections can be important in the diagnosis of absolute impurity concentrations in fusion plasma modeling, as well as in Auger electron spectroscopy, and electron-energy-loss spectroscopy [1]. *K*-shell ionization cross sections of Ni [2], Cu [3], Fe, and Mn [4], and *L*-shell ionization cross sections of W [5], have all been measured using a thin-target technique. Corrections for the influence of the substrate have been made to these measurements [6].

Ab initio theoretical calculations for such processes are scarce. Most recent theoretical attention for ionization of heavy atoms has focused on ionization of the valence electrons, using perturbative methods. Also, many previous calculations of *K*-shell and *L*-shell ionization cross sections have been made for highly charged systems [7–9], where most of the electrons have already been stripped. For these cases, relativistic distorted-wave calculations have been shown to be accurate for a wide range of targets. These studies have allowed simple (yet accurate) fits to be made to the ionization cross sections, which have proven extremely useful in many plasma modeling applications [10]. These studies have also shown that purely relativistic effects [9] become important for large impact energies and for high-Z systems, where Z is the nuclear charge.

In this paper we study the inner-shell ionization of heavy neutral targets using relativistic distorted-wave techniques for several reasons. First, we wish to assess the accuracy of a distorted-wave approach for calculating inner-shell ionization cross sections from a neutral target of high-Z value. It is well known that distorted-wave calculations for ionization of valence electrons [11,12] from near-neutral, moderate-Z and high-Z targets are often inaccurate, due to the incomplete treatment of the electron-electron correlations between the incident, outgoing, and bound electrons. However, as will be shown, the case of inner-shell ionization can be accurately described using distorted-wave techniques, most likely because the incident electron interacts only slightly with the valence electrons due to its large energy. Currently, none of the existing nonperturbative theoretical techniques such as the convergent close-coupling method, the *R* matrix with pseudostates approach, or time-dependent close-coupling method (see e.g., Ref. [13]), which all generally give accurate results for valence-shell ionization, have been extended to examine inner-shell ionization processes. This deficiency is no doubt due to the extreme complexity of describing fully the interaction of an incident electron with *all* electrons of a heavy target, which would be required for a fully nonperturbative approach to the inner-shell ionization process.

Second, we wish to make comparisons with existing experimental measurements to gauge the accuracy of such measurements. The accuracy of previous measurements has been unclear due to a lack of detailed theoretical calculations for these processes, and previous comparisons have only been made with classical scaling calculations [14] or with scaled Born calculations [15]. Finally, we note that there have been recent empirical model calculations proposed which give *K*-shell ionization cross sections for a large range of atomic targets [16]. Although these fits are often very useful, it is still important to have detailed *ab initio* quantal calculations to verify the accuracy of such fits and to further explore the physics inherent in the scattering process.

Our paper proceeds as follows. In the next section we discuss our theoretical approach to calculating the inner-shell ionization of Mn, Fe, Ni, Cu, and W. In Sec. III we compare our theoretical calculations with existing experimental measurements for the inner-shell ionization cross sections of selected heavy atoms and discuss our results. We end with a short conclusion.

II. METHOD

A. Theoretical techniques

In this work we follow closely the techniques for calculating relativistic distorted-wave cross sections as discussed by Sampson and co-workers [7–9,17,18]. These methods are currently available as part of the suite of Los Alamos atomic data codes. The Los Alamos codes used to carry out the present calculations were the semirelativistic structure code CATS [19], the fully relativistic Dirac-Fock-Slater structure code RATS [20,21], and the multipurpose ionization code GIPPER [22]. We now give a brief summary of our fully relativistic distorted-wave method.

The electron-impact ionization process is defined as

$$e^- + |\beta_t J_t\rangle \rightarrow e^{-\prime} + e^{-\prime\prime} + |\beta_t'' J_t''\rangle, \tag{1}$$

where J_t is the total angular momentum of the level in the initial N-electron atom, and J_t'' is the total angular momentum

of the level in the final $(N-1)$-electron ion. The quantities β_t and β_t'' are used to represent all other quantum numbers required to completely define the initial and final levels, respectively. The relativistic distorted-wave cross section for this process is given by

$$Q(\beta_t J_t - \beta_t'' J_t'') = \frac{8a_0^2}{k^2 g_i} \sum_J (2J+1) \sum_{J_t'} \sum_{\kappa,\kappa',\kappa''} \int_0^{(\epsilon - I)/2} \times d\epsilon'' |\langle \Psi_i | \sum_{\substack{q,p \\ q<p}}^{N+1} \frac{1}{r_{qp}} | \Psi_f \rangle|^2, \quad (2)$$

where a_0 is the Bohr radius and k is the relativistic wave number of the impact electron, related to the kinetic energy ϵ of the impact electron by

$$k^2 = \epsilon \left[1 + \frac{\alpha^2}{4} \epsilon \right], \quad (3)$$

with α being the fine structure constant and with ϵ in Rydbergs. In Eq. (2), J is the total angular momentum of the entire system, and J_t' is the total final angular momentum for the system consisting of the $(N-1)$-electron final ion with total angular momentum J_t'' plus the ejected electron with total angular momentum j''. The quantity I is the ionization potential between levels $|\beta_t J_t\rangle$ and $|\beta_t'' J_t''\rangle$, ϵ'' is the energy of the ejected electron, and g_i is the statistical weight of the initial level of the N-electron target atom. The κ in Eq. (2) represents the usual relativistic quantum number which is related to the orbital and total angular momentum quantum numbers l and j for the partial-wave expansion of the impact-electron wave function by

$$\kappa = l, \quad j = l - \frac{1}{2}; \quad \kappa = -(l+1), \quad j = l + \frac{1}{2}. \quad (4)$$

Similar expressions hold for the scattered (κ') and ejected (κ'') electron quantum numbers.

The initial antisymmetrized function Ψ_i for the $(N+1)$-electron system can be written as

$$\Psi_i = \frac{1}{(N+1)^{1/2}} \sum_{k=1}^{N+1} (-1)^{N+1-k} \times \sum_{M_t,m} C(J_t j M_t m; JM) \Psi_{\beta_t J_t}(x_k^{-1}) u_{\epsilon l j m}(x_k), \quad (5)$$

where x_k represents the space and spin coordinates of electron k and x_k^{-1} means the space and spin coordinates for all N electrons other than k. The function $\Psi_{\beta_t J_t}(x_k^{-1})$ is the initial antisymmetrized target-atom wave function constructed of Dirac spinors or orbitals [17]. The quantity $u_{\epsilon l j m}$ is a Dirac spinor that represents a partial wave for the initial free electron with kinetic energy ϵ in the presence of a central potential $V(r)$ resulting from the target ion

$$u_{\epsilon l j m}(x) \equiv u_{\epsilon \kappa m}(x) = \frac{1}{r} \begin{bmatrix} P_{\epsilon\kappa}(r) \chi_{\kappa m}(\theta, \phi, \sigma) \\ i Q_{\epsilon\kappa}(r) \chi_{-\kappa m}(\theta, \phi, \sigma) \end{bmatrix}, \quad (6)$$

where the $\chi_{\kappa m}$ are the usual spin angular momentum functions, and the large and small components of the radial functions $P_{\epsilon\kappa}$ and $Q_{\epsilon\kappa}$ satisfy the coupled Dirac equations

$$\left(\frac{d}{dr} + \frac{\kappa}{r} \right) P_{\epsilon\kappa}(r) = \frac{\alpha}{2} \left[\epsilon - V(r) + \frac{4}{\alpha^2} \right] Q_{\epsilon\kappa}(r), \quad (7)$$

and

$$\left(\frac{d}{dr} - \frac{\kappa}{r} \right) Q_{\epsilon\kappa}(r) = -\frac{\alpha}{2} [\epsilon - V(r)] P_{\epsilon\kappa}(r). \quad (8)$$

In these equations the central potential $V(r)$ is chosen to be the Dirac-Fock-Slater potential given (in Rydbergs) by

$$V(r) = \frac{-2Z}{r} + V_c(r) - \left(\frac{24\rho}{\pi} \right)^{1/3}, \quad (9)$$

where

$$V_c(r) = \sum_{n'\kappa'} w_{n'\kappa'} \int_0^\infty \frac{2}{r_>} [P_{n'\kappa'}^2(r_1) + Q_{n'\kappa'}^2(r_1)] dr_1, \quad (10)$$

and

$$\rho(r) = \frac{1}{4\pi r^2} \sum_{n'\kappa'} w_{n'\kappa'} [P_{n'\kappa'}^2(r) + Q_{n'\kappa'}^2(r)]. \quad (11)$$

Here $w_{n'\kappa'}$ is the occupation number of subshell $n'\kappa' = n'l'j'$ in the initial configuration of the N-electron target atom, the summation is over all occupied subshells, $r_>$ is the greater of r and r_1, and $P_{n'\kappa'}$ and $Q_{n'\kappa'}$ are the large and small components of the radial function of a bound electron in the $n'\kappa'$ subshell. These bound orbital functions are obtained from a pair of coupled equations very similar to Eqs. (7) and (8), except that the system is treated as an eigenvalue problem for the bound orbitals.

The final, $(N+1)$-electron, antisymmetrized function Ψ_f in Eq. (2) can be written in a form that is very similar to the expression for Ψ_i appearing in Eq. (5). Specifically

$$\Psi_f = \frac{1}{(N+1)^{1/2}} \sum_{k=1}^{N+1} (-1)^{N+1-k} \times \sum_{M_t',m'} C(J_t' j' M_t' m'; JM) \Psi_{\beta_t' J_t'}(x_k^{-1}) u_{\epsilon' l' j' m'}(x_k), \quad (12)$$

where the primed quantities pertain to the scattered electron wave function and the N-electron system comprised of the final bound level and the ejected free electron. The function $\Psi_{\beta_t' J_t'}(x_k^{-1})$ contains an extra free-electron spinor (associated with the ejected electron) and is given by

$$\Psi_{\beta_t' J_t'}(x_k^{-1}) = \frac{1}{N^{1/2}} \sum_{p \neq k}^{N+1} (-1)^{N-p} \sum_{M_t'', m''} C(J_t'' j'' M_t'' m''; J_t' M_t') \times \Psi_{\beta_t'' J_t''}(x_p^{-1}) u_{\epsilon'' l'' j'' m''}(x_p), \quad (13)$$

where $\Psi_{\beta_t'' J_t''}$ is the antisymmetrized wave function corresponding to the final $(N-1)$-electron ion with total angular momentum J_t'' and $u_{\epsilon'' l'' j'' m''}(x_p)$ is a Dirac spinor for the ejected electron with kinetic energy ϵ''. The P and Q radial functions that comprise the scattered and ejected spinor functions (u) appearing in Eqs. (12) and (13) are determined from a set of coupled Dirac equations that are identical in form to Eqs. (7) and (8). The only difference is that the central potential $V(r)$ is now obtained from the bound electron orbitals that represent the appropriate configurations of the final $(N-1)$-electron ion. We also note that the normalization for any of the free electron wave functions is chosen to be

$$\int_0^\infty [P_{\epsilon\kappa}(r) P_{\epsilon'\kappa}(r) + Q_{\epsilon\kappa}(r) Q_{\epsilon'\kappa}(r)] dr = \pi \delta(\epsilon - \epsilon'). \quad (14)$$

In the heavy atoms under consideration in this study, ionization of a K-shell or L-shell electron leads to a final state that could be described by numerous fine-structure levels. Calculations which consider ionization to each of these levels would take a prohibitively large amount of time to complete. Consequently, we instead consider ionization from a configuration-average approach [23], which makes the calculations much more tractable. We expect this simplification to be a very good approximation for ionization from the K or L subshells. The configuration-average transition can be written symbolically as

$$e^- + |\cdots n\kappa^w \cdots\rangle \rightarrow e^{-\prime} + e^{-\prime\prime} + |\cdots n\kappa^{w-1} \cdots\rangle, \quad (15)$$

where $n\kappa$ represents the active subshell containing w electrons. The cross section describing this process can be obtained from Eq. (1) by taking the appropriate average over all initial and sum over all final target levels, $|\beta_t J_t\rangle$ and $|\beta_t'' J_t''\rangle$, that belong to initial and final configurations, $c = |\cdots n\kappa^w \cdots\rangle$ and $c'' = |\cdots n\kappa^{w-1} \cdots\rangle$, respectively. If there is no mixing present in these initial and final states and, furthermore, if the ionization energy for each of the possible state to state transitions can be approximated by a single configuration-average ionization energy, I^{CA}, then the configuration-average cross section can be expressed in the simple form

$$Q^{\mathrm{CA}}(n\kappa^w) \equiv Q^{\mathrm{CA}}(c - c'') = \sum_{\substack{\beta_t J_t \in c \\ \beta_t'' J_t'' \in c''}} g_{\beta_t J_t} Q(\beta_t J_t - \beta_t'' J_t'')/g_c, = w Q_{\mathrm{H}}^{\mathrm{ps}}(n\kappa), \quad (16)$$

where g is the statistical weight of the appropriate state or configuration. The pseudohydrogenic cross section, $Q_{\mathrm{H}}^{\mathrm{ps}}(n\kappa)$, is merely the cross section that would result from Eq. (2) if one were to consider ionization of the lone $n\kappa$ electron from a hydrogenic ion with ionization potential I^{CA}. However, the $n\kappa$ wave function to be used in Eq. (2) is that obtained from the relevant N-electron target, rather than from a hydrogenic target.

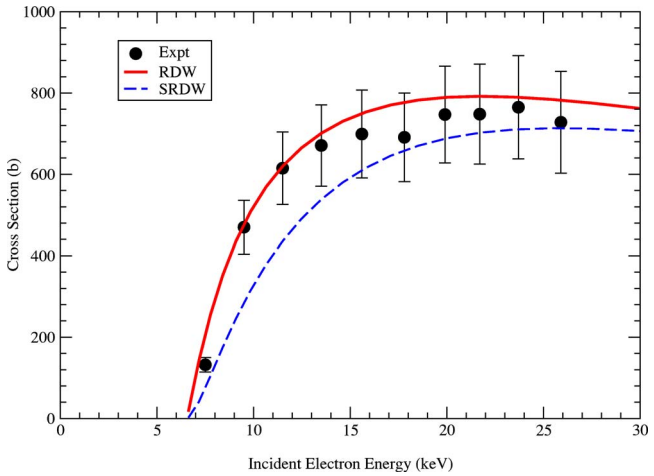

FIG. 1. (Color online) K-shell electron-impact ionization of Mn. We compare the relativistic distorted-wave (RDW) calculations with our experimental measurements. The dashed curve is a semirelativistic distorted-wave (SRDW) calculation.

In our calculations, the RATS structure code was used to generate fully relativistic bound electron wave functions for the ground configuration of the neutral target and for the excited (relativistic) configurations of the singly charged ion with either a $1s_{1/2}$, $2s_{1/2}$, $2p_{1/2}$, or $2p_{3/2}$ electron removed. The GIPPER code was then used to compute the ionization cross sections using the method described above. We also used the CATS structure code to generate semirelativistic bound-electron wave functions which, in turn, were used to generate free-electron wave functions and ionization cross sections in the GIPPER code. The calculations of the bound-electron wave functions use Cowan's HFR method [23], which includes the mass-velocity and Darwin operators explicitly within the appropriate differential equations. However, the free-electron wave functions include semirelativistic effects only to the extent that the wave functions are computed from a central potential derived from the bound electron orbitals. There is no explicit account taken of semirelativistic corrections in the free-electron function equations.

III. RESULTS AND DISCUSSION

Comparison of our theoretical calculations with existing experimental measurements for the inner-shell $1s_{1/2}$ ionization of four neutral targets are shown in Figs. 1–4, for the atoms Mn, Fe, Ni, and Cu, respectively. Although recent papers on K-shell ionization [16] have presented cross sections for extremely wide energy ranges, we choose to focus here on the near threshold range, since that is where the experimental measurements were made, and since the region near the peak of the curve is often the most important part of the ionization cross section when calculating ionization rate coefficients for typical plasma conditions.

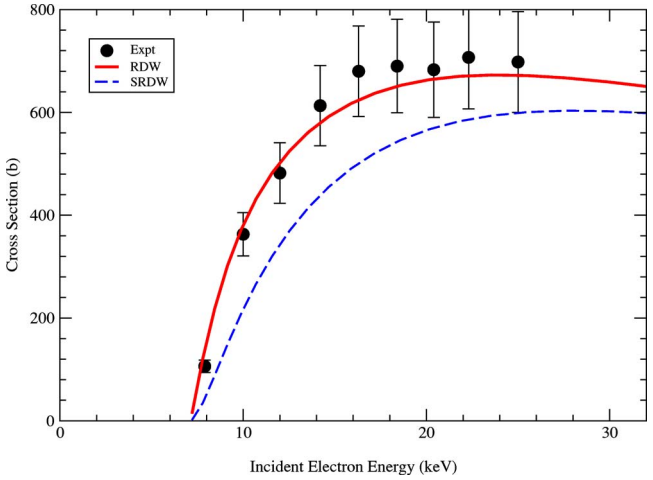

FIG. 2. (Color online) K-shell electron-impact ionization of Fe. We compare the RDW calculations with our experimental measurements. The dashed curve is a SRDW calculation.

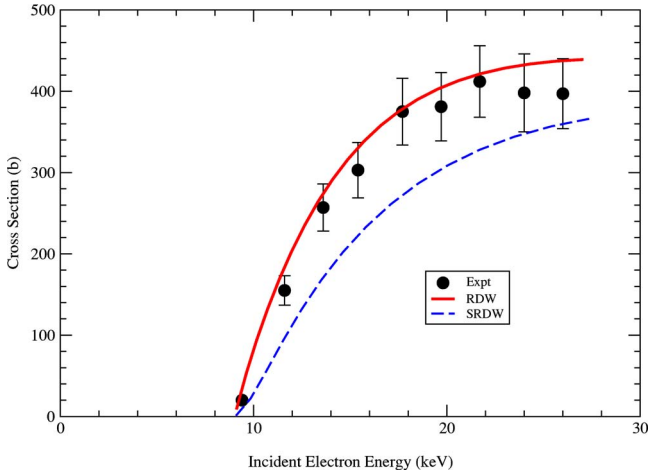

FIG. 4. (Color online) K-shell electron-impact ionization of Cu. We compare the RDW calculations with our experimental measurements. The dashed curve is a SRDW calculation.

For these targets it is clear that the relativistic distorted-wave calculations are in excellent agreement with the measurements. In all cases the calculations go through the error bars of the measurements, and in most cases the calculations are very close to the actual experimental points. We find this agreement quite remarkable, since previous experience indicates that distorted-wave calculations for ionization of valence electrons from neutral targets often over estimate the ionization cross section. The good agreement leads us to postulate the following description of the inner-shell ionization process. It appears that the high energy of the impacting electron makes any interaction between itself and the valence electrons very small. The fast impact electron quickly finds itself feeling the potential due to two tightly bound $1s$ electrons and the heavy nucleus. The impact electron ionizes one of these $1s$ electrons and is itself scattered. Within this framework it is not so surprising that a distorted-wave type theory could accurately describe such a process, since it is well known that distorted-wave calculations are usually quite accurate for calculations of ionization of highly charged systems.

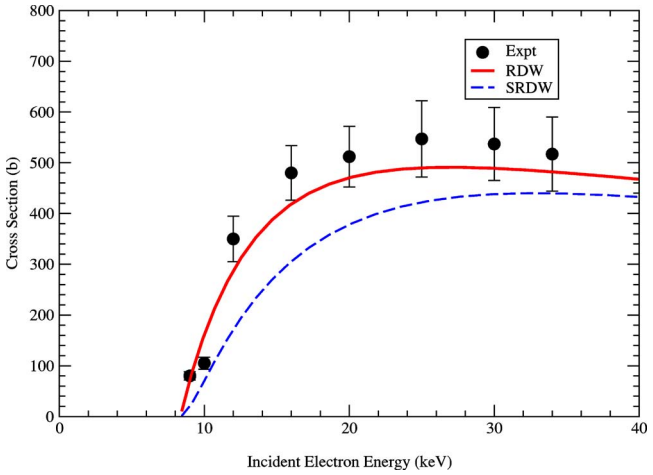

FIG. 3. (Color online) K-shell electron-impact ionization of Ni. We compare the RDW calculations with our experimental measurements. The dashed curve is a SRDW calculation.

Furthermore, the distortion potential $V(r)$ has the correct limiting behavior when the impact electron is both far away (no field) and at the point of closest approach to the nucleus (the appropriate Coulombic potential of the form $-2(Z-N)/r$ where $N\sim 2$ for $1s$ ionization). In between these extremes, the distortion potential is probably not very accurate, because the electron-electron correlation between the bound and free electrons is treated only to first order. However, it appears that the high energy of the impacting electron renders it relatively insensitive to the details of the distortion potential in this intermediate region. A similar argument holds for the scattered and ejected electrons, provided we are far enough from threshold that the ejected and scattered electrons do not spend a significant amount of time near the spectating bound electrons.

It is also interesting to explore how much of the ionization cross section is influenced by relativistic effects. To investigate this behavior, we carried out semirelativistic distorted-wave calculations for the $1s$ ionization of the same four cases, as described previously. These calculations are shown by the dashed lines in Figs. 1–4. It is clear that use of the Dirac-Fock-Slater potential, and the fully relativistic treatment of both bound and free radial wave functions, makes a significant difference to the ionization cross section, even though the semirelativistic calculations have almost the same ionization threshold as the fully relativistic calculations. The semirelativistic calculations are consistently lower than the relativistic distorted-wave calculations (and, for most cases, outside the error bars of the experimental measurements), and strongly suggests that for these types of ionizing collisions, a fully relativistic description is needed to adequately describe the scattering process.

Finally, in Fig. 5 we present the L-shell ionization of W; that is, the total of the $2s_{1/2}$, $2p_{1/2}$, and $2p_{3/2}$ inner-shell ionization cross sections. For this case, the agreement between experiment and theory is reasonably good in the near-threshold region where the calculations are only slightly

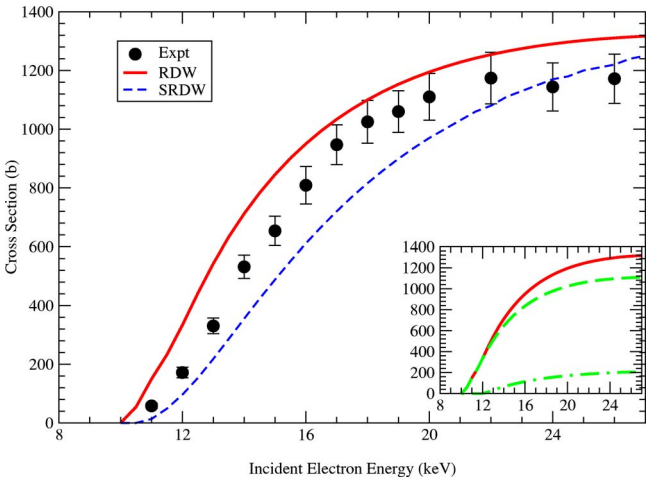

FIG. 5. (Color online) *L*-shell electron-impact ionization of W. We compare the RDW calculations with our experimental measurements. The dashed curve is a SRDW calculation. In the inset figure, the dot-dashed line and the long-dashed line represent the contributions to the total ionization cross section from the $2s_{1/2}$ and the $2p_{1/2}+2p_{3/2}$ subshells, respectively.

higher than experiment for a range of impact energies leading up to the peak of the cross section. Again, for this case, the semirelativistic distorted-wave calculations (dashed line) are somewhat lower than the fully relativistic calculations. We also examined the contribution to the total *L*-shell ionization cross section from the individual $2s_{1/2}$ and $2p_{1/2}+2p_{3/2}$ shells (see inset). The trends of the $2s_{1/2}$ and $2p_{1/2}+2p_{3/2}$ ionization cross sections are very similar to the total ionization cross section, with the $2p$ ionization providing the dominant contribution.

IV. CONCLUSIONS

In this paper, we have presented theoretical calculations of inner-shell ionization of heavy neutral targets and compared with existing experimental measurements. Generally, very good agreement is found between the relativistic distorted-wave calculations and measurements made using a thin-target technique. We postulate that this good agreement implies that the valence electrons play little role in this deep inner-shell ionization process, and that this description explains the accurate predictions of the relativistic distorted-wave calculations. We have also found that relativistic effects do play an important role in these ionization processes, and must be fully taken into account when describing both bound-electron and free-electron wave functions in order to calculate accurate cross sections.

ACKNOWLEDGMENTS

We acknowledge useful discussions with J. Abdallah. We thank Z. Luo and Z. An for communication of their experimental measurements, and for useful discussions concerning these measurements. This work was performed under the auspices of the U.S. Department of Energy through the Los Alamos National Laboratory.

[1] C. J. Powell, in *Electron Impact Ionization*, edited by T. D. Märk and G. H. Dunn (Springer-Verlag, New York, 1985), Chap. 6.
[2] Z. Luo, Z. An, F. He, T. Li, X. Long, and X. Peng, J. Phys. B **29**, 4001 (1996).
[3] Z. An, T. H. Li, L. M. Wang, X. Y. Xia, and Z. M. Luo, Phys. Rev. A **54**, 3067 (1996).
[4] Z. Luo, Z. An, T. Li, L. Wang, Q. Zhu, and X. Xia, J. Phys. B **30**, 2681 (1997).
[5] D. L. Yang, X. B. Luo, Y. C. Fu, F. Q. He, X. G. Long, X. F. Peng, and Z. M. Luo, Chin. Phys. **13**, 670 (2004).
[6] Z. M. Luo, Phys. Rev. B **32**, 812 (1985).
[7] C. J. Fontes, D. H. Sampson, and H. L. Zhang, Phys. Rev. A **48**, 1975 (1993).
[8] C. J. Fontes, D. H. Sampson, and H. L. Zhang, At. Data Nucl. Data Tables **72**, 217 (1999).
[9] C. J. Fontes, D. H. Sampson, and H. L. Zhang, Phys. Rev. A **59**, 1329 (1999).
[10] C. J. Fontes, J. Abdallah, Jr., R. E. H. Clark, and D. P. Kilcrease, J. Quant. Spectrosc. Radiat. Transf. **65**, 223 (2000).
[11] J. Colgan, S. D. Loch, M. S. Pindzola, C. P. Ballance, and D. C. Griffin, Phys. Rev. A **68**, 032712 (2003).
[12] S. D. Loch, J. A. Ludlow, M. S. Pindzola, A. D. Whiteford, and D. C. Griffin, Phys. Rev. A **72**, 052716 (2005).
[13] S. D. Loch, M. Witthoeft, M. S. Pindzola, I. Bray, D. V. Fursa, M. Fogle, R. Schuch, P. Glans, C. P. Ballance, and D. C. Griffin, Phys. Rev. A **71**, 012716 (2005).
[14] M. Gryzinski, Phys. Rev. **115**, 374 (1959).
[15] E. J. McGuire, Phys. Rev. A **16**, 73 (1977).
[16] A. K. F. Haque, M. A. Uddin, A. K. Basak, K. R. Karim, and B. C. Saha, Phys. Rev. A **73**, 012708 (2006).
[17] H. L. Zhang and D. H. Sampson, Phys. Rev. A **42**, 5378 (1990).
[18] D. H. Sampson, H. L. Zhang, A. K. Mohanty, and R. E. H. Clark, Phys. Rev. A **40**, 604 (1989).
[19] J. Abdallah, R. E. H. Clark, and R. D. Cowan, Los Alamos National Laboratory, Los Alamos Manual No. LA 11436-M-I, 1988; http://aphysics2.lanl.gov/tempweb/
[20] J. Abdallah, Jr., R. E. H. Clark, D. P. Kilcrease, G. Csanak, and C. J. Fontes, *Atomic Processes in Plasmas*, edited by A. L. Osterheld and W. H. Goldstein, AIP Conf. Proc. No. 381 (AIP, Woodbury, NY, 1996).
[21] J. Abdallah, Jr., H. L. Zhang, C. J. Fontes, D. P. Kilcrease, and B. J. Archer, J. Quant. Spectrosc. Radiat. Transf. **71**, 107 (2001).
[22] R. E. H. Clark, J. Abdallah, and J. B. Mann, Astrophys. J. **381**, 597 (1991); B. J. Archer, R. E. H. Clark, C. J. Fontes, H. L. Zhang, Los Alamos Memorandum LA-UR-02-1526, 2002.
[23] R. D. Cowan, *The Theory of Atomic Structure and Spectra* (University of California Press, Berkeley, 1981).